

Simplicial Multivalued Maps and the Witness Complex for Dynamical Analysis of Time Series

Zachary Alexander, Elizabeth Bradley, James D. Meiss, and Nicole Sanderson

Departments of Computer Science, Applied Mathematics & Mathematics
University of Colorado
Boulder, CO 80309-0526

December 3, 2024

Abstract

Topology based analysis of time-series data from dynamical systems is powerful: it potentially allows for computer-based proofs of the existence of various classes of regular and chaotic invariant sets for high-dimensional dynamics. Standard methods are based on a cubical discretization of the dynamics, and use the time series to construct an outer approximation of the underlying dynamical system. The resulting multivalued map can be used to compute the Conley index of isolated invariant sets of cubes. In this paper we introduce a discretization that uses—by contrast—a simplicial complex constructed from a witness-landmark relationship. The goal is to obtain a natural discretization that is more tightly connected with the invariant density of the time series itself. The time-ordering of the data also directly leads to a map on this simplicial complex that we call the witness map. We obtain conditions under which this witness map gives an outer approximation of the dynamics, and thus can be used to compute the Conley index of isolated invariant sets. The method is illustrated by a simple example using data from the classical Hénon map.

1 Introduction

Our goal in this paper is to develop methods for characterizing some aspects of a dynamical system, discrete or continuous, using computational topology. We assume that the only knowledge we have of the dynamics is a finite time series $\Gamma = \{x_0, x_1, \dots, x_{T-1}\}$ taken from a state-space trajectory of the system. If the system is a map, $f : X \rightarrow X \subset \mathbb{R}^n$, then Γ is simply the iterates of the map: $x_{t+1} = f(x_t)$. If the system is a flow, then Γ is a sequence of samples of the continuous trajectory $x(t)$ and we are effectively studying the evolution operator that maps the system forward in time. In either case, given this information, we cannot hope to approximate the dynamics on all of X ; instead, we assume that f has an attractor Λ , and that Γ lies close to Λ . Thus our goal is to characterize properties of $f|_{\Lambda}$ such as the number and types of periodic orbits, and whether the dynamics is chaotic on Λ .

The tool that we use is the Conley index of an isolating neighborhood of f [Eas98, KMM04]. Recall that a set K is isolating if the subset that remains in K for all time, i.e., an isolated invariant set of f relative to this neighborhood, is contained in its interior: $\text{inv}(K) \subset \text{int}(K)$. The Conley index can be used to characterize the dynamical properties of isolated invariant sets within K —for example it may establish the existence of periodic orbits or give a lower bound on the topological entropy.

The computation of the Conley index relies on the construction of an *index pair* [MM02]:

Definition (Index Pair). A pair of compact sets (N, E) with $E \subset N \subset X$ is called an *index pair* for $S = \text{inv}(N \setminus E)$ if it satisfies the following three properties, illustrated in Fig. 1:

- $\text{cl}(N \setminus E)$ is an isolating neighborhood.
- $f(E) \cap N \subseteq E$.
- $f(N \setminus E) \subset N$.

The first property above states that the set $K = \text{cl}(N \setminus E)$ is an isolating neighborhood that isolates some (possibly empty) invariant set S . The second property implies that once a trajectory enters E , it will not return to K before leaving the index pair entirely. The third property states that E contains the exit set of N : that is, the images of points not in E must remain in N .

For any index pair, a continuous map f_N can be defined on the space N/E by

$$f_N(x) = \begin{cases} f(x), & \text{if } x, f(x) \in N \setminus E \\ [E], & \text{otherwise} \end{cases}$$

This map, in turn, induces an equivalence class of maps, $[f_{N*}]$, on the homology group $H_*(N, E)$ of N relative to E . The equivalence class—maps that are shift equivalent—is the Conley index $\text{Con}(S, f)$ of the invariant set S isolated by K . The simplest implication is that whenever $\text{Con}(S, f) \neq [0]$, then $S \neq \emptyset$ [KMM04, Thm 10.91]. In addition, periodic orbits are guaranteed when the “Lefschetz number” is nonzero [KMM04, Thm 10.46], and—for C^∞ maps—the topological entropy is positive whenever the shift equivalence class of f_{N1} has spectral radius greater than one [Bak02].

One of the fundamental advantages of the Conley index is its structural stability; for example, if K is an isolating neighborhood for f , then there is $\epsilon > 0$ such that K is also an isolating neighborhood for \tilde{f} , whenever $\|f - \tilde{f}\|_\infty < \epsilon$. Moreover, so long as an invariant set remains isolated by K , its Conley index does not change [MM02].

Since we only have access to the trajectory Γ , we must use this orbit to obtain an approximation of the underlying dynamics before we can compute the Conley index. There are two categories of maps that can serve this purpose. The first, as we recall in §2, are multivalued maps. These are set-valued and typically defined on a finite covering of a neighborhood of the attractor Λ ; they capture how the images of the cover map across other elements of the cover. Multivalued maps have most commonly been defined on cubical grids [MMSR97, MMRS99], but more-general grids can also be used. Members of this more-general class of maps, which we call *cellular multivalued maps* (CMMs), are defined to be constant on the interior of each cell. Note that while connectivity is obvious in uniform grids of cubical cells, that may not be the case in other grid geometries. The second category of map addresses this issue. Dual to any grid, cubical or otherwise, is a cell complex—the

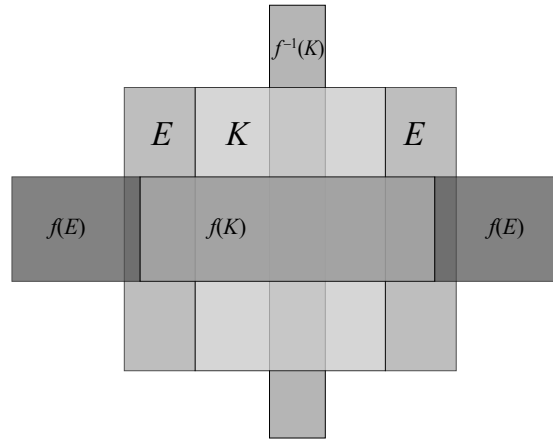


Figure 1: An index pair $N = K \cup E$ (a square) and E (two rectangles). The image of E either leaves N or remains in E . For this picture the isolating neighborhood K is guaranteed to contain a fixed point. A simple map with this index pair is $f(x, y) = (ax, by)$ with $a > 1 > b > 0$.

nerve of the grid. A CMM induces a map on this dual complex. When the number of grid cells is finite, such maps are finitely representable: they can be stored precisely in a computer and used to perform exact computations. The associated computational cost depends on the geometry of the cells. To minimize this complexity while still preserving the essential features, our approach uses two constructions that play major roles in computational topology: the α -diagram [EM92, Ede95] and the *witness complex* [dSC04].

The α -diagram of a data set is the intersection of its Voronoi diagram with the union of balls of radius α centered on the data points. The nerve of the α -diagram is the α -complex: it is generically a simplicial complex and is a subset of the Delaunay triangulation, limiting to the latter as $\alpha \rightarrow \infty$ [Ede95]. We call the map induced on this complex by the dynamics a *simplicial multivalued map* or SMM. If an index pair can be found for a multivalued map, the Conley index can be computed using the corresponding CMM or SMM. Moreover, if the cellular map is semicontinuous and *acyclic*, then its homology coincides with that of f , and thus it can be used to compute the Conley index of isolated invariant sets of f .

Since the geometry of cells in the α -diagram is dictated by the data, rather than by rectilinear grid lines, the shape of the α -complex naturally follows the shape of the attractor Λ . This flexible, data-driven representation provides a major computational advantage over the uniform cubical complex, which in practice almost always contains many empty cells that must be accounted for in the algorithms that track the associated multivalued map. Even so, the α -complex is still computationally challenging. Every point in the time series $\Gamma = \{x_0, x_1, \dots, x_{T-1}\}$ is a vertex of at least one simplex, and the complexity of algorithms that construct and manipulate these objects scales poorly with the number of simplices.

It is useful, then, to represent these data using a global topological object that contains fewer simplices while preserving the Conley index. We use the *witness complex* [dSC04] for this purpose. Instead of assigning a vertex in the complex to each point in Γ , we represent the data by a smaller set of vertices, a set of *landmarks*, $L \subset X$, and build a simplicial complex from those points. As

described in §2.1, there are a number of ways to choose landmarks. Associated with (Γ, L) is a witness relation: each point in Γ may be a witness to one or more landmarks and each landmark may have one or more witnesses. There are many possible definitions of the witness relation. We use one in which a point in Γ witnesses a set σ of landmarks if it is closer to all of the landmarks in σ than the remaining landmarks and the distance between the point and any landmark in σ is within ϵ of the minimum distance between the point and the set of landmarks. We use this witness relation to construct an abstract simplicial complex, the *witness complex*. The simplest implementation gives a clique or flag complex: it consists of simplices whose pairs of vertices have a common witness. The parameter ϵ can be used to define a persistent homology [ZC05]—and ultimately, we conjecture, a persistent Conley index.

In order to capture the dynamics, we construct a pair of *witness maps*: a cellular multivalued map induced on the α -cells by the time-series data and the corresponding simplicial multivalued map on the witness complex. These maps, which are a primary contribution of this paper, are described in §3. We develop their construction in several steps in order to bring the well-developed theory of [KMM04] to bear upon this new formulation and thereby establish the correspondence between the homology of the witness map and that of the true dynamics of the underlying system. For data generated from the classic Hénon map, we show that, under a verifiable set of assumptions, our techniques can be used to obtain rigorous results about the underlying dynamical system.

2 Multivalued Maps

In this section we describe the concept of *cellular multivalued map*, a generalization of the cubical multivalued map of [KMM04]. We begin by recalling some standard definitions for multivalued maps that approximate a dynamical system¹.

Definition (Multivalued Map). A *multivalued map*, denoted $F : X \rightrightarrows X$, is a map from a topological space X , to its power set. That is, for each $x \in X$, $F(x)$ is a subset of X .

We use multivalued maps to approximate continuous maps $f : X \rightarrow X$, and the approximation is taken to be “good” if the homology of F is equivalent to that of f . In order for this to be the case, the action of F must *enclose* the action of f and not introduce any extra homological structure. These requirements are spelled out in the following definitions.

Definition (Outer Approximation). A multivalued map $F : X \rightrightarrows X$ is an *outer approximation* of a continuous map $f : X \rightarrow X$ if $f(x) \in F(x)$ for each $x \in X$. In this case f is said to be a *continuous selector* for F .

The (weak) preimage of a multivalued map is itself a multivalued map defined as

$$F^{-1}(y) = \{x \in X : y \in F(x)\}.$$

Definition (Semicontinuous). A multivalued map is (lower) *semicontinuous* if the preimage of each open set is open.

¹Following [DJM04, DFT08], we denote single-valued maps with lower-case letters (e.g., f), sets and set-valued maps with capital letters, e.g., F , and combinatorial objects and maps with calligraphic letters, e.g. \mathcal{F} .

As usual, the n -dimensional homology group of a set X is denoted $H_{*n}(X)$. We use, for simplicity, the homology over \mathbb{Z}_2 so that the torsion subgroups are ignored. Given this, a multivalued map preserves homology if the image of each point is homologous to a point.

Definition (Acyclic). A multivalued map F is *acyclic* if for each $x \in X$,

$$H_{*n}(F(x)) = \begin{cases} \mathbb{Z}_2, & n = 0 \\ \mathbf{0}, & n > 0 \end{cases}$$

When F is semicontinuous and acyclic, F is said to be an *enclosure* of f . The key point is that if F is semicontinuous and acyclic, then every continuous selector for F induces the same homomorphism in homology—a consequence of the acyclic carrier theorem [Mun84, Thm. 13.3]. Therefore, one can define the homology of an enclosure F to be the homology of any of its continuous selectors.

In order that this homology be computable, however, it is necessary to obtain a finitely representable approximation of the map f , and it is this to which we turn next.

2.1 Grids and α -Complexes

A grid allows one to construct finitely representable maps that are outer approximations of a map f [KMV05, Mro99]. Instead of the cubical grids of [KMM04], we use a grid constructed from an α -complex. Many of the results that appear here are easily adapted from the cubical case.

Definition (Grid [AKK+09]). A family of nonempty compact sets \mathcal{A} is called a *grid* on a topological space X if:

- a) $X = \bigcup_{A \in \mathcal{A}} A$;
- b) for all $A \in \mathcal{A}$, $A = \text{cl}(\text{int}(A))$;
- c) for all $A, B \in \mathcal{A}$ if $A \neq B$ then $A \cap \text{int}(B) = \emptyset$; and
- d) a finite subset of \mathcal{A} covers each compact $S \subset X$.

A prototypical grid is a lattice of closed cubes; indeed, this is the example studied extensively in [KMM04]. Though cubical grids lead to simple algorithms, they have the disadvantage of being less parsimonious than other choices.

We construct our grid using the α -diagram of a finite set, $L = \{l_1, \dots, l_\ell\} \subset X$, of *landmarks*. The landmarks should be selected to cover the time series Γ with some accuracy: there should be a landmark within some prescribed distance from each element of Γ . They should also be relatively sparse: the minimal distance between any two should not be too small. These two requirements are linked, as will be discussed in §3. A simple selection method, advocated by [dSC04], is to choose the landmarks from Γ itself by a “max-min” algorithm: choose L iteratively by selecting the farthest point in Γ from the previous selection until the operative density and sparseness requirements are satisfied, if possible. For the simple example in §4, we choose the landmarks uniformly in X . More generally, the problem of finding the most appropriate landmarks in an efficient way is an interesting question for future investigation.

Once the landmarks are selected, a grid can be constructed from α -cells centered at the landmark points. Recall that an α -cell at l_i is the intersection of the closed ball of radius α , $B_\alpha(l_i)$, with the Voronoi cell of l_i :

$$A_i(\alpha) = B_\alpha(l_i) \cap \{x \in X : d(x, l_i) \leq d(x, L)\}, \quad (1)$$

where $d(x, y)$ is a metric on X , and the distance from x to a subset $S \subset X$ is $d(x, S) = \inf_{y \in S} d(x, y)$. An example of a set of landmarks and their associated α -cells is shown in Fig. 2.

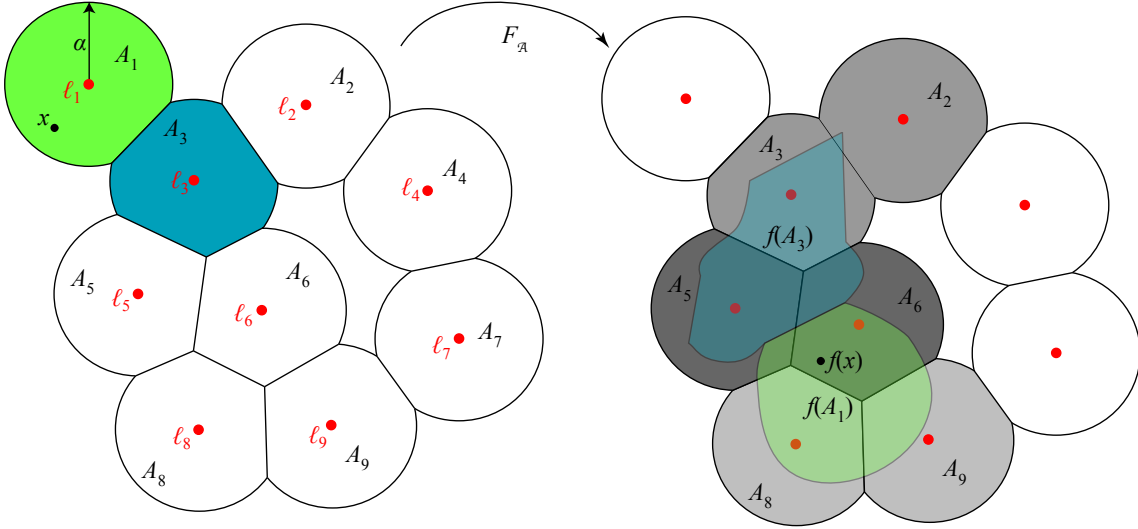


Figure 2: Sketch of a grid \mathcal{A} of α -cells based on a set of nine landmarks $\{l_i\}$ (red points) and the action of a cellular map $F_{\mathcal{A}}$ on two of these cells. Here the image of any $x \in \text{int}(A_1)$ is $A_5 \cup A_6 \cup A_8 \cup A_9$ and of any $x \in \text{int}(A_3)$ is $A_2 \cup A_3 \cup A_5 \cup A_6$. If $x \in A_1 \cap A_3$ then $F_{\mathcal{A}}(x) = A_5 \cup A_6$.

There are a number of objects associated with the α -diagram. The first is simply the collection of cells, $\mathcal{A} = \{A_1, A_2, \dots, A_\ell\}$. The second is the geometrical realization of this collection—the union of these cells as subsets of \mathbb{R}^n —denoted by

$$|\mathcal{A}| := \bigcup_{A \in \mathcal{A}} A. \quad (2)$$

With this definition it is straightforward to show that the collection of α -cells is a grid:

Lemma 1. *A set of α -cells is a grid on $|\mathcal{A}|$.*

This lemma allows us to use results based on the similar notion of a cubical multivalued map [KMM04]. The only difference between the α -cell and cubical cases is the shape of the grid cells. The advantage of α -cells over cubes is more flexibility in geometry and topology—and more efficiency in computation.

2.2 Cellular and Simplicial Maps

A cellular multivalued map is a map on the geometrical realization of a grid \mathcal{A} that is constant on the interior of each cell of a grid. It generalizes the cubical multivalued map of [KMM04], since the inter-cell boundaries no longer need to be rectilinear.

Definition (Cellular Multivalued Map (CMM)). A cellular multivalued map $F_{\mathcal{A}} : |\mathcal{A}| \rightrightarrows |\mathcal{A}|$ on the realization of a grid \mathcal{A} is the outer approximation of f defined by

$$F_{\mathcal{A}}(x) := \bigcap_{B \in \mathcal{A}} \{A \in \mathcal{A} : A \cap f(B) \neq \emptyset, x \in B\} \quad (3)$$

A cellular multivalued map takes the interior of each cell to the union of the cells that its image intersects, and takes the boundary shared by multiple cells to the intersection of their images. An implication is that cellular multivalued maps are semicontinuous because they map the boundary of each cell to a subset of the image of the cell itself, a generalization of [KMM04, Prop. 6.17] for the related cubical case. The map $F_{\mathcal{A}}$ is a multivalued map on the metric space $|\mathcal{A}|$. An example is shown in Fig. 2, where the image of any point x in the interior A_1 , for example, is the union of the cells A_5, A_6, A_8 , and A_9 .

Even though this construction gives us an intuitive understanding of the map, it is not easy to implement on a computer, for two reasons: it is a map on an infinite space $|\mathcal{A}|$, and to construct it we must know $f(x)$ for each point $x \in |\mathcal{A}|$. The first problem is mitigated by defining a finite map $\mathcal{F} : \mathcal{K} \rightrightarrows \mathcal{K}$, on a complex \mathcal{K} related to the grid \mathcal{A} . One such complex is the CW-complex formed from \mathcal{A} : that is, the collection of cells $\{A_i\}$, together with their faces obtained from intersections $\{A_i \cap A_j\}$, and so forth. An example is the cubical CW-complex used in the approach of [KMM04]. Since the cellular map $F_{\mathcal{A}}$ is constant on each cell derived from \mathcal{A} , it naturally gives rise to an associated combinatorial map. In the example of Fig. 2, the 2-cell A_1 is mapped to $\{A_5, A_6, A_8, A_9\}$ and the 1-cell represented by $A_1 \cap A_3$ is mapped to $\{A_5, A_6\}$.

Our goal is to use a more easily described complex that is also naturally suited to homology calculations: in particular, a simplicial complex. Recall that an abstract simplicial complex \mathcal{K} is a set of finite, ordered subsets $\sigma = \langle l_{i_0}, \dots, l_{i_p} \rangle$ in the power set, 2^L , of a set of vertices L such that if $\tau \leq \sigma$ is a “face” of σ , then it is also a simplex in \mathcal{K} . The vertices, $\langle l_i \rangle$, are zero-simplices; edges, $\langle l_i, l_j \rangle$, are one-simplices, etc. The empty set is a face of every simplex.

Since our grid is a collection of α -cells, the natural simplicial complex to use is the α -complex, defined as the *nerve* of \mathcal{A} ; for example, the nerve of the grid in Fig. 2 is shown in Fig. 3. Each vertex in the nerve of \mathcal{A} corresponds to the center l_i of an α -cell A_i , and each edge $\langle l_i, l_j \rangle$ to a face $A_i \cap A_j \neq \emptyset$. More generally, for a p -simplex $\sigma = \langle l_{i_0}, \dots, l_{i_p} \rangle$, let

$$A_{\sigma}(\alpha) := \bigcap_j \{A_j(\alpha) \in \mathcal{A} : l_j \in \sigma\} \subset |\mathcal{A}|, \quad (4)$$

denote the intersection of the cells whose centers form the vertices of the simplex σ . The α -complex is then

$$\mathcal{K}_{\alpha} := \{\tau \in 2^L : A_{\tau}(\alpha) \neq \emptyset\} \cup \emptyset. \quad (5)$$

Alternatively $\sigma \in \mathcal{K}_{\alpha}$ if there exists an open ball $B_r(x_0)$ with $r < \alpha$ that contains no vertices in L , $B_r(x_0) \cap L = \emptyset$, but for which $\sigma \subset \partial B_r(x_0)$. The boundary of such a ball is called a *circumsphere* of σ . The α -complex is always an abstract simplicial complex. However, it may not be geometrically embedded in \mathbb{R}^n , unless the vertices l_i are in “general position”—that is, at most $n + 1$ vertices lie on a circumsphere [Ede95]. We assume this is the case, and so the simplices in \mathcal{K} have maximal dimension $n = \dim(X)$.

The cellular multivalued map $F_{\mathcal{A}}$ induces a combinatorial map $\mathcal{F}_{\mathcal{K}} : \mathcal{K} \rightarrow \mathcal{K}$ that is defined to commute with the correspondence between the α -grid and the α -complex.

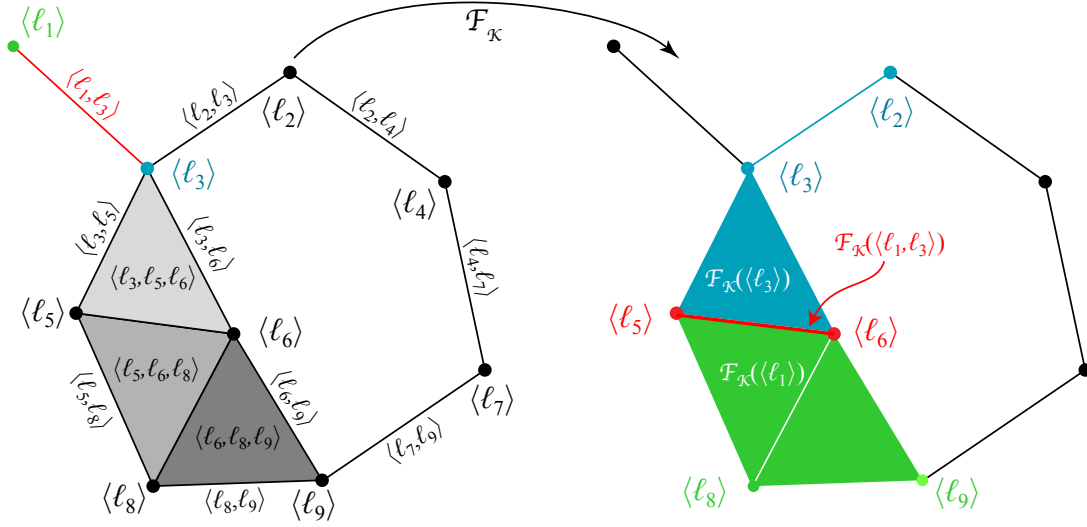


Figure 3: Simplicial complex \mathcal{K} that is the nerve of the α -cells of Fig. 2, and the action of the simplicial map $\mathcal{F}_{\mathcal{K}}$, induced by $F_{\mathcal{A}}$, on the simplices $\langle l_1 \rangle$ (green), $\langle l_3 \rangle$ (blue) and $\langle l_1, l_3 \rangle$ (red).

Definition (Simplicial Multivalued Map (SMM)). A simplicial map $\mathcal{F}_{\mathcal{K}} : \mathcal{K} \rightrightarrows \mathcal{K}$ is defined by

$$\mathcal{F}_{\mathcal{K}}(\sigma) := \{\tau : A_{\tau} \subset F_{\mathcal{A}}(A_{\sigma})\}. \quad (6)$$

where $F_{\mathcal{A}}$ is the cellular map (3) on the α -grid \mathcal{A} and $\sigma \in \mathcal{K}$ is a simplex in the nerve of \mathcal{A} .

Note that $\mathcal{F}_{\mathcal{K}}$ is a combinatorial multivalued map: its domain consists of simplices and its range of sets of simplices, and that each set $\mathcal{F}_{\mathcal{K}}(\sigma)$ is a subcomplex of \mathcal{K} . As an example, the map $\mathcal{F}_{\mathcal{K}}$ induced by the cellular map of Fig. 2 is shown in Fig. 3. In this case, since $A_{\langle l_1 \rangle} = A_1$, then $\{\langle l_5, l_6, l_8 \rangle, \langle l_6, l_8, l_9 \rangle\} \subset \mathcal{F}_{\mathcal{K}}(\langle l_1 \rangle)$ as are the nine faces of these two 2-simplices. Similarly, since $A_{\langle l_1, l_3 \rangle} = A_1 \cap A_3$, then $\mathcal{F}_{\mathcal{K}}(\langle l_1, l_3 \rangle) = \{\langle l_5, l_6 \rangle, \langle l_5 \rangle, \langle l_6 \rangle\}$.

Definition (6) above satisfies the closed graph condition:

Lemma 2 (Closed Graph Condition). *If $\mathcal{F}_{\mathcal{K}}$ is an SMM and $\tau \leq \sigma \in \mathcal{K}$ (i.e., τ is a face of σ), then $\mathcal{F}_{\mathcal{K}}(\tau) \supset \mathcal{F}_{\mathcal{K}}(\sigma)$.*

Proof. Since $\tau \leq \sigma$, then by (4) $A_{\tau} \supset A_{\sigma}$. The definition (3) implies that $F_{\mathcal{A}}(A_{\tau}) \supset F_{\mathcal{A}}(A_{\sigma})$, and so by (6) $\mathcal{F}_{\mathcal{K}}(\tau) \supset \mathcal{F}_{\mathcal{K}}(\sigma)$. \square

Just as a simplicial map is constructed from the nerve of a grid, a cellular map can be constructed on the geometrical realization of the simplicial complex. For each $\sigma \in \mathcal{K}$, let $|\sigma| \in \mathbb{R}^n$ be the convex hull of its vertices and $|\mathcal{K}|$ be the union its geometrical simplices. Note that $|\mathcal{K}| \subset |\mathcal{A}|$ because each α -cell is convex. The map $F_{\mathcal{K}} : |\mathcal{K}| \rightrightarrows |\mathcal{K}|$ is the multivalued map induced by $\mathcal{F}_{\mathcal{K}}$; i.e., by analogy with (3):

$$F_{\mathcal{K}}(x) := \bigcap_{\sigma \in \mathcal{K}} \{|\tau| : \tau \in \mathcal{F}_{\mathcal{K}}(\sigma), x \in |\sigma|\} \quad (7)$$

The nerve theorem states that the nerve of a finite collection of closed convex sets is homotopy equivalent to the union of the collection [BT82, Wu62]. In our case, this means that $|\mathcal{K}| \simeq |\mathcal{A}|$. The homotopy equivalence between \mathcal{A} and \mathcal{K} implies there exists a deformation retract, a continuous $R : |\mathcal{A}| \times [0, 1] \rightarrow |\mathcal{A}|$, with $R(x, 0) = x$, $R(x, 1) = r(x) \in |\mathcal{K}|$, and $r(x) = x$ for $x \in |\mathcal{K}|$. We make the reasonable assumption that, since the α -cells are convex, r can be chosen to preserve inclusion in the specific α -cells; that is, if $x \in A_i$, then $r(x) \in A_i$.

Our goal is now to show that $F_{\mathcal{A}}$ and $F_{\mathcal{K}}$ contain the same information about homology. To show this, we begin with the following ‘‘partial commutativity’’ lemma.

Lemma 3. *Let \mathcal{A} , \mathcal{K} , $F_{\mathcal{A}}$, and $F_{\mathcal{K}}$ be defined as above and let $R : \mathcal{A} \times [0, 1] \rightarrow \mathcal{A}$ be a deformation retract. Let $r : \mathcal{A} \rightarrow \mathcal{K}$ be defined as $r(x) := R(x, 1)$ and suppose that $r(A_i) \subset A_i$. Then for any $x \in \mathcal{A}$, $(F_{\mathcal{K}} \circ r)(x) \subseteq (r \circ F_{\mathcal{A}})(x)$.*

Proof. Note that since r is onto $|\mathcal{K}|$ and is the identity on $|\mathcal{K}|$, $r(A_i) = |\mathcal{K}| \cap A_i$ and it suffices to show that for any $x \in |\mathcal{A}|$, $F_{\mathcal{K}}(r(x)) \subseteq F_{\mathcal{A}}(x)$. Furthermore, we note that it follows directly from (6) that for any simplex $\tau \in \mathcal{K}$, $|\mathcal{F}_{\mathcal{K}}(\tau)| \subseteq F_{\mathcal{A}}(A_{\tau})$. For an $x \in |A_{\tau}|$, $r(x)$ is a point in a geometric simplex $|\tau|$. Therefore, by (7),

$$F_{\mathcal{K}}(r(x)) \subseteq |\mathcal{F}_{\mathcal{K}}(\tau)| \subseteq F_{\mathcal{A}}(A_{\tau})$$

as required. □

This result is exactly what is needed to show that the homologies of $F_{\mathcal{K}}$ and $F_{\mathcal{A}}$ are isomorphic. In particular, we can prove the following:

Theorem 4. *Whenever $F_{\mathcal{A}}$ is an acyclic multivalued map, then $F_{\mathcal{K}}$ induces the same map on homology as $F_{\mathcal{A}}$.*

Proof. Whenever $F_{\mathcal{A}}$ is an acyclic multivalued map, then the definition (6) implies that $F_{\mathcal{K}}$ is as well. Moreover, since R is a deformation retract, r_* is the identity; thus, the maps $r \circ F_{\mathcal{A}}$ and $F_{\mathcal{K}} \circ r$ are also acyclic. Now, by Lem. 3, $F_{\mathcal{K}} \circ r$ is a submap of $r \circ F_{\mathcal{A}}$; therefore, it follows that there is a continuous map $u : \mathcal{A} \rightarrow \mathcal{K}$ that is a continuous selector for both $F_{\mathcal{K}} \circ r$ and $r \circ F_{\mathcal{A}}$. Thus, if v and w are continuous selectors for $F_{\mathcal{K}}$ and $F_{\mathcal{A}}$, respectively, then $(v \circ r)$ and $(r \circ w)$ are continuous selectors carried by $(F_{\mathcal{K}} \circ r)$ and $(r \circ F_{\mathcal{A}})$. The acyclic carrier theorem [Mun84, Thm. 13.3] then implies that

$$(v \circ r)_* = u_* = (r \circ w)_* \quad \Rightarrow \quad v_* \circ r_* = r_* \circ w_* \quad \Rightarrow \quad v_* = w_*.$$

□

By (3), $F_{\mathcal{A}}$ is semicontinuous and an outer approximation of f ; therefore, if $F_{\mathcal{A}}$ is acyclic, it induces a well-defined map in homology such that $(F_{\mathcal{A}})_* = f_*$. That is, in order to determine the Conley index of f , we need only to know the homology of the multivalued map $F_{\mathcal{A}}$ and check acyclicity. Note that our construction of the cellular multivalued map, $F_{\mathcal{A}}$, is still purely theoretical: knowledge of the points in a time series does not mean that one knows the map f on every point in the phase space, and thus one cannot compute the outer approximation. Without this, there is no direct method to compute the associated simplicial map $\mathcal{F}_{\mathcal{K}}$ on the nerve. In §3 we define a map—the witness map—that can be computed algorithmically from time-series data. We then

provide a set of conditions under which the witness map and the cellular map contain the same information about homology. These results allow us to calculate the Conley index of f using $F_{\mathcal{W}}$ rather than $F_{\mathcal{A}}$. Below, we first develop the theoretical framework and algorithms to compute the Conley index with respect to $F_{\mathcal{A}}$.

2.3 Conley Index of $F_{\mathcal{A}}$

In order to use the Conley index to obtain information about f , we start by using $F_{\mathcal{A}}$ to locate isolating neighborhoods for f . Since the construction of the CMM is analogous to the cubical map of [KMM04], we borrow the presentation as well as relevant theorems and algorithms from that work and from [DFT08]. In most cases, the proofs of the theorems in this section are identical to those in the original citations if one simply substitutes the concept of an α -cell for that of a cube. A thorough treatment of the cubical-grid versions of these results—with respect to any grid satisfying the first definition in Section 2.1—can be found in [Mro99]. Our goal is to move beyond the cubical complexes used in previous work and devise a method to *efficiently* build a *simplicial* multivalued map that contains the same information as the cellular multivalued map.

We begin by defining trajectories and invariant sets for the multivalued map, following [DFT08].

Definition (Combinatorial Trajectory). A *combinatorial trajectory* of $F_{\mathcal{A}}$ through $A \in \mathcal{A}$ is a bi-infinite sequence of α -cells, $\Gamma_A = (\dots, A^{(-1)}, A^{(0)}, A^{(1)}, \dots)$, such that $A^{(0)} = A$ and $A^{(n+1)} \subseteq F_{\mathcal{A}}(A^{(n)})$ for all $n \in \mathbb{Z}$.

Definition (Combinatorial Invariance). Given a cellular multivalued map $F_{\mathcal{A}} : |\mathcal{A}| \rightrightarrows |\mathcal{A}|$, the *combinatorial invariant part* of $N \subset \mathcal{A}$ is defined by

$$\text{inv}(N, F_{\mathcal{A}}) := \{A \in \mathcal{A} : \exists \text{ a trajectory } \Gamma_A \subset N\}$$

The following algorithm can be used to locate the combinatorial invariant part of a compact set N .

Algorithm 5. *invariantPart*($N, F_{\mathcal{A}}$)

```

 $S \leftarrow N$ 
repeat
   $S' \leftarrow S$ 
   $S \leftarrow F_{\mathcal{A}}(S) \cap S \cap F_{\mathcal{A}}^{-1}(S)$ 
until  $S = S'$ 
return  $S$ 

```

It is proved in [KMM04, Thm 10.83]—in the context of cubical sets—that if N is finite this algorithm terminates and returns $\text{inv}(N, F_{\mathcal{A}})$ (which could be empty). The extension to the cellular case is straightforward.

Associated with this notion of invariance, there is a property of isolation, which is defined using:

Definition (Combinatorial Neighborhood). The *combinatorial neighborhood* of a set $S \subset \mathcal{A}$ is

$$o(S) := \{B \in \mathcal{A} : B \cap S \neq \emptyset\}.$$

More plainly, the combinatorial neighborhood consists of S and all of the α -cells that touch its boundary. In order for a combinatorial invariant set to be isolated, it must be the invariant set of some neighborhood.

Definition (Combinatorial Isolating Neighborhood). A set $K \subset \mathcal{A}$ is a *combinatorial isolating neighborhood* if

$$o(\text{inv}(K, F_{\mathcal{A}})) \subseteq K$$

Given a guess, K , for such a neighborhood, we might be able to find an isolating one by *growing* it: if $K' = \text{inv}(o(K), F_{\mathcal{A}}) \subset K$, then K is isolating, otherwise we replace K by K' and repeat. For example, in §4 where we are looking for a fixed point, we use the α -cell containing a nearly recurrent point as the initial guess. This leads to the algorithm of [DFT08]:

Algorithm 6. *growIsolating*($K, F_{\mathcal{A}}$)

```

while  $\text{inv}(o(K), F_{\mathcal{A}}) \not\subseteq K$  do
   $K \leftarrow \text{inv}(o(K), F_{\mathcal{A}})$ 
  if  $K \cap \partial|\mathcal{A}| \neq \emptyset$  then
    return  $\emptyset$ 
  end if
end while
return  $K$ 

```

If *growIsolating* is called with a combinatorial set $K \subset \mathcal{A}$ and a cellular multivalued map $F_{\mathcal{A}}$, then it returns a combinatorial isolating neighborhood for $F_{\mathcal{A}}$ —or else it fails when K intersects the boundary of the grid \mathcal{A} . A sufficient condition for this not to occur is that $|\mathcal{A}|$ is itself an isolating neighborhood because then each α -cell that touches the boundary of $|\mathcal{A}|$ has a neighborhood whose invariant part is contained in $|\mathcal{A}|$.

An important point is that when K is isolating for $F_{\mathcal{A}}$, then under certain conditions, $|K|$ is isolating for any continuous selector f of $F_{\mathcal{A}}$:

Theorem 7. *Let $F_{\mathcal{A}} : |\mathcal{A}| \rightrightarrows |\mathcal{A}|$ be a cellular multivalued map for f . Then if $K \subset \mathcal{A}$ is a combinatorial isolating neighborhood for $F_{\mathcal{A}}$, $|K|$ is an isolating neighborhood for f .*

This is essentially [KMM04, Thm 10.87], generalized to the cellular case.

The computation of the Conley index for a cellular multivalued map begins with an isolating neighborhood K , with the goal of finding a pair of sets (N, E) that satisfy the definition of an index pair for the cellular map. We compute these using the following algorithm.

Algorithm 8. *indexPair*($K, F_{\mathcal{A}}$)

```

 $S \leftarrow \text{inv}(K, F_{\mathcal{A}})$ 
 $C \leftarrow o(S) \setminus S$ 
 $E \leftarrow F_{\mathcal{A}}(S) \cap C$ 
repeat
   $E' \leftarrow E$ 
   $E \leftarrow F_{\mathcal{A}}(E) \cap C \cap E'$ 
until  $E = E'$ 
 $N \leftarrow S \cup E$ 
return  $(N, E)$ 

```

This is similar to Alg. 10.86 in [KMM04] which was stated for cubical sets. It was proven there that if this algorithm is called with a combinatorial isolating neighborhood K and an outer approximation

$F_{\mathcal{A}}$ of f , then the geometric realization of the pair it returns is an index pair for f . This proof can be adapted to the cellular-map situation.

Having computed an index pair $(|N|, |E|)$ for f , we are ready to compute the Conley index. For this, we need to compute $f_* : H_*(|N|, |E|) \rightarrow H_*(|N|, |E|)$. However as mentioned before, we do not wish to use the CW-complex generated from \mathcal{A} , nor the map $F_{\mathcal{A}}$ because of their complexity. Instead we compute a different map that we call a *witness map* and show that it has the same homology as $F_{\mathcal{A}}$.

3 The Witness Complex and Map

In this section, we describe a method for computing a simplicial complex \mathcal{W} that is a variant of the *witness complex* of [dSC04], together with an associated *witness map* $\mathcal{F}_{\mathcal{W}}$ on that complex that captures the action of the dynamics on \mathcal{W} . We assume that the only information that we have is a time series $\Gamma = \{x_0, \dots, x_{T-1}\}$ that corresponds to a trajectory near an attractor $\Lambda \subset X$ of a dynamical system f , e.g., $f(x_t) = x_{t+1}$. The guiding philosophy here is that if we were to choose the set L of vertices for the α -complex as the entire orbit, $L = \Gamma$, then when $T \gg 1$, it would be prohibitively expensive to compute α -cells and the associated map $F_{\mathcal{A}}$. However, we can more easily compute a simplicial complex relative to a much smaller set of landmarks $L = \{l_1, \dots, l_\ell\}$ that are near Γ . As mentioned in §2.1, one strategy is to choose $L \subset \Gamma$ by the max-min procedure of [dSC04]; however, there are many other possible methods, and indeed it is not necessary to select L as a subset of Γ . For each $\alpha \geq 0$, the set L corresponds to a grid of α -cells by (1).

Once the landmarks are selected, the remainder of the data serves as a set of “witnesses,” which together define a witness complex \mathcal{W} . Through the temporal ordering of the orbit, these witnesses also define an associated map $\mathcal{F}_{\mathcal{W}}$ on this complex. Below, we show that if the data satisfy certain density criteria and the landmarks are (more or less) uniformly spaced, then the homology of \mathcal{W} coincides with that of an α -complex defined on the same set of landmarks. Moreover, when f is Lipschitz, we show that there is an α such that $\mathcal{F}_{\mathcal{W}}$ induces a map $F_{\mathcal{W}}$ on the α -cells of L that carries the same information as both $F_{\mathcal{A}}$ and $\mathcal{F}_{\mathcal{K}}$. In §4, we show how to implement these requirements in an example.

3.1 Witness Complex

Following a general construction of Dowker [Dow52], a witness complex is an abstract simplicial complex that is defined by a relation—that is, by the selection of a subset:

$$W_R \subset \Gamma \times L, \tag{8}$$

the *witness relation*. We say a point $x \in \Gamma$ is a witness to a point $l \in L$ if $(x, l) \in W_R$. Thus,

$$W(l) = \{x \in \Gamma : (x, l) \in W_R\}$$

is the set of witnesses to a landmark. There are many possible choices for the witness relation W_R . For example, according to de Silva and Carlsson, a point x is a *weak* witness to $\{l_0, \dots, l_p\}$ if the $p + 1$ nearest neighbors in L to x are $\{l_0, \dots, l_p\}$. If, in addition, x is equidistant from each of the l_i , then it is a *strong* witness [dSC04]. We choose to define a witness relation that balances

these ideas: x is a witness to a set of $p + 1$ landmarks $\{l_0, \dots, l_p\}$ if each landmark l_i is within ϵ of the minimal distance between x and the set of landmarks. For this case, the set of witnesses to a landmark l is:²

$$W_\epsilon(l) := \{x_t \in \Gamma : d(x_t, l) \leq d(x_t, L) + \epsilon\}. \quad (9)$$

Here, ϵ can be thought of as representing the *fuzziness* of the boundary between cells. The definition (9) becomes the strong witness relation for $\epsilon = 0$.

One witness complex associated with a relation W_R corresponds to the simplices whose vertices share a witness—that is, σ is a simplex when the set $W(\sigma) = \bigcap_{l \in \sigma} W(l)$ is not empty. A more easily computed version of the witness complex is a clique complex (the “lazy” complex of [dSC04]). Recall that a *clique* (or *flag*) complex is the maximal complex with a given set of edges [Zom10]; for example, the Vietoris-Rips complex is a clique complex. For a given witness relation, the clique complex is the complex defined by

$$\mathcal{W}(\Gamma, L) = \{\sigma : W(l) \cap W(l') \neq \emptyset, \forall l, l' \in \sigma\}. \quad (10)$$

Note that, though the vertices of each edge in σ must share a witness, there need not be a single witness to every vertex in the simplex.

An example is shown in Fig. 4 for an orbit of the logistic map on $[0, 1]$ for a parameter value just above the first period-doubling accumulation point. Here, the landmarks were selected to be every 30th point in the sorted data, an orbit of length 300. The relation $W_R \subset \Gamma \times L$ is the set of the points near the diagonal (blue). For the case shown, each point in Γ is a witness to at most two landmarks, and so the maximum dimension of a simplex in the complex (10) is one.

One way to compute the sets defined in (9) is to sort the rows of the $T \times \ell$ distance matrix $D_{tj} = \|x_t - l_j\|$ in order of increasing size, i.e., for the sorted matrix $D_{t,1}^s = d(x_t, L)$. Then x_t is a witness to all of the landmarks in the first few columns of the t^{th} row of D^s , namely those for which $D_{t,j}^s \leq D_{t,1}^s + \epsilon$. The main computational expense here—the distance calculations—can be reduced using a *kd*-tree [FBF77]. Note that to find a p -dimensional simplex one need only find the $k = p + 1$ nearest neighbors, which reduces the memory requirements (viz., storing the matrix). In addition, most implementations of efficient k -nearest-neighbors algorithms return their results sorted in size order.

The following section describes how the complex $\mathcal{W}_\epsilon(\Gamma, L)$ using the witness relation (9) can be related to the α -complex.

3.2 Equivalence Conditions for \mathcal{K}_α and \mathcal{W}_ϵ

Since the witness complex is based on the set of landmarks L that form the centers of the α -grid, then for large enough α , $|\mathcal{W}_\epsilon(\Gamma, L)| \subset |\mathcal{A}_\alpha(L)|$. Moreover, for large enough α , the associated α -complex \mathcal{K}_α is a clique complex, just as we have assumed for \mathcal{W}_ϵ in (10). We will show here that when this is the case—and if the landmarks are not too closely spaced—then $\mathcal{W}_\epsilon \subset \mathcal{K}_\alpha$. Moreover, when the data Γ are dense enough on $|\mathcal{A}_\alpha|$, then we will see that $\mathcal{K}_\alpha \subset \mathcal{W}_\epsilon$. Thus, when both sets of conditions are satisfied, the complexes are the same. As the hypotheses to obtain these results are independent, we state these two results separately.

²In the notation of [dSC04], this relation corresponds to the complex $W(D, \epsilon, 1)$, where D denotes the matrix of distances between landmarks and witnesses.

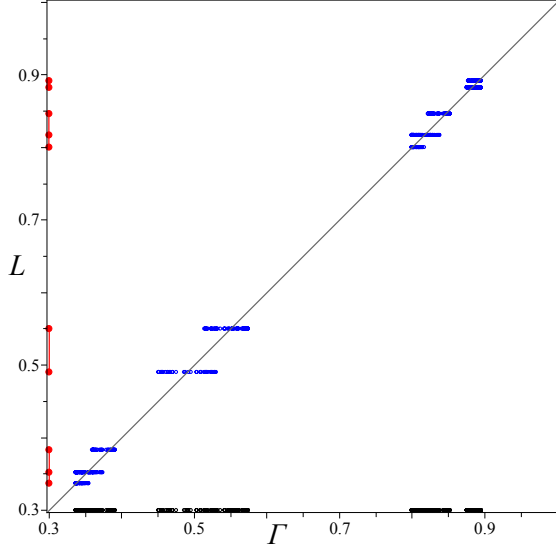


Figure 4: Witnesses (blue points) defined by the relation (9) for the logistic map, $f(x) = 3.56x(1-x)$ with $\epsilon = 0.01$. The orbit Γ , shown along the horizontal axis (black points), has $T = 300$ points, and there are $\ell = 10$ landmarks, shown along the vertical axes (red points). The witness relation defines six, one-dimensional simplices (the line segments along the vertical axis), giving a complex with $\beta_0 = 4$. These correspond to the four major bands in the chaotic attractor of f .

Theorem 9. *Let $\mathcal{K}_\alpha(L)$ be the α -complex (5) and $\mathcal{W}_\epsilon(\Gamma, L)$ be the witness complex (10) associated with a set of landmarks L and a time series Γ . Furthermore, suppose that there is a $\delta \leq \epsilon/2$ such that Γ is δ -dense on $|\mathcal{A}_\alpha|$. Then $\mathcal{K}_\alpha \subseteq \mathcal{W}_\epsilon$.*

Proof. Suppose $\sigma \in \mathcal{K}_\alpha$, i.e., there is a $y \in |\mathcal{A}|$ such that $\Delta = d(y, L) = \|y - l_i\| \leq \alpha$ for all $l_i \in \sigma$. We want to show that there is an $x \in \Gamma$ such that $x \in W_\epsilon(\sigma)$. Since Γ is δ -dense, for any $y \in |\mathcal{A}|$, there is at least one point $x \in \Gamma \cap B_\delta(y)$. Since $d(y, L) = \Delta$ and $\|x - y\| \leq \delta$, it follows that

$$d(x, L) \geq \Delta - \delta.$$

Then, since $x \in B_\delta(y)$,

$$\|x - l_i\| \leq \Delta + \delta \leq d(x, L) + 2\delta \leq d(x, L) + \epsilon, \quad l_i \in \sigma,$$

since $\delta \leq \epsilon/2$. Hence, $x \in W_\epsilon(l_i)$ for each vertex of σ and therefore, $\sigma \in \mathcal{W}_\epsilon$. \square

Note that this theorem applies even when the witness complex is not defined as a clique complex. However, to show the converse—as we do next—requires the clique assumption.

Theorem 10. *Suppose $\mathcal{K}_\alpha(L)$ and $\mathcal{W}_\epsilon(\Gamma, L)$ are as in Thm. 9, and define*

$$M = \max_{x \in \Gamma} d(x, L) \quad \text{and} \quad \beta = \min_{i \neq j} \|l_i - l_j\|.$$

If α is chosen so that

$$M + \epsilon \leq \alpha \leq \frac{\beta}{\sqrt{2}}, \tag{11}$$

and so that \mathcal{K}_α is a clique complex, then $\mathcal{W}_\epsilon \subseteq \mathcal{K}_\alpha$.

Proof. Note that \mathcal{K}_α and \mathcal{W}_ϵ have the same vertex set. Furthermore, by assumption each complex is a clique complex. This means that \mathcal{K}_α and \mathcal{W}_ϵ are each determined completely by their edges. It follows that we only need to verify that every edge in \mathcal{W}_ϵ is also an edge in \mathcal{K}_α .

Supposing that $\langle l_1, l_2 \rangle \in \mathcal{W}_\epsilon$, then these landmarks share a witness, i.e., there is an $x \in \Gamma$ such that $\|x - l_i\| \leq d(x, L) + \epsilon$ for $i \in \{1, 2\}$. We want to show that there is a point $y \in |\mathcal{A}|$ such that $\|y - l_1\| = \|y - l_2\| = \Delta = d(y, L) \leq \alpha$. Since $\|l_1 - l_2\| \leq 2d(x, L) + 2\epsilon$, then if y is the midpoint of the segment joining l_1 and l_2 ,

$$\Delta \leq d(x, L) + \epsilon \leq M + \epsilon \leq \alpha,$$

by (11). Let $l_3 \in L$ be next closest landmark to y , besides l_1 and l_2 , and define $\beta_1 = \|l_3 - l_1\|$, and $\beta_2 = \|l_3 - l_2\|$. By assumption $\beta_i \geq \beta$ and thus, as illustrated in Fig. 5, $\Delta' = \|l_3 - y\|$ is minimized when $\beta_1 = \beta_2 = \beta$. In this case, the segment from l_3 to y is the perpendicular bisector of the segment from l_1 to l_2 and so we have $\Delta \leq \Delta'$ only if $\Delta \leq \frac{\beta}{\sqrt{2}}$. Since $\Delta \leq \alpha$, this condition is assured by (11), and it follows that $\langle l_1, l_2 \rangle \in \mathcal{K}_\alpha$, and, since \mathcal{K}_α is a clique complex, that $\mathcal{W}_\epsilon \subseteq \mathcal{K}_\alpha$. \square

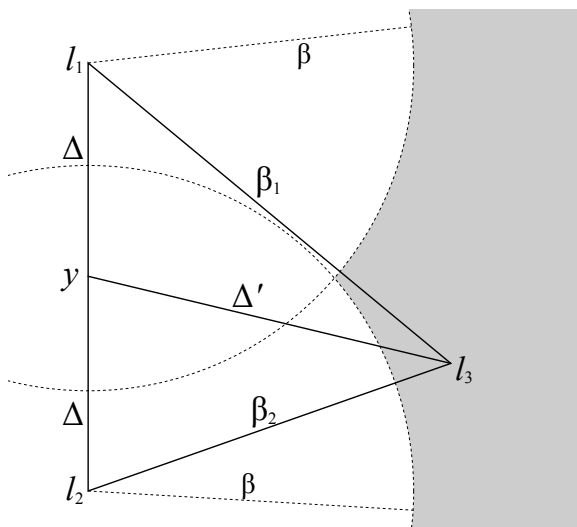


Figure 5: An illustration of the spacing between three landmarks l_1, l_2 , and l_3 , as in the proof of Thm. 10. The point y is the midpoint between the two landmarks l_1 and l_2 . By assumption, the distance from l_3 to l_1 or l_2 is at least β , and it is thus minimized when $\beta_1 = \beta_2 = \beta$.

In order to apply Thm. 10, \mathcal{K}_α must be a clique complex, and this is typically not true for all $\alpha \geq 0$. However, since the Delaunay complex, \mathcal{D} , is a clique complex (the Voronoi cells cover \mathbb{R}^d); then $\mathcal{K}_\infty = \mathcal{D}$ is a clique complex as well. Indeed, whenever α is larger than the radius of the biggest circumsphere that defines an n -dimensional simplex in \mathcal{D} , then $\mathcal{K}_\alpha = \mathcal{D}$. For the simple case of a hexagonal array of landmarks in \mathbb{R}^2 , these circumcircles all have radius $\beta/\sqrt{3}$, so it is easy to determine when \mathcal{K}_α is clique. Finally, for the trivial case when $\alpha < \beta/2$, the α -balls about each landmark are disjoint, so the α -complex is trivial, and also a clique complex.

When both Thm. 9 and Thm. 10 hold, then $\mathcal{W}_\epsilon = \mathcal{K}_\alpha$. In this case, a map defined using the witness relation may have the same homology as a map on \mathcal{A} . It is to this issue that we turn next.

3.3 Witness Map

Abstractly, we can define a multivalued map on a grid $|\mathcal{A}|$ defined by the landmarks L using the witness relation: whenever $x \in A_i$ and there is a witness x_t to the landmark l_i , then the image of x should include the cells that x_{t+1} witnesses. The appropriate map is defined in the same way as the cellular map $F_{\mathcal{A}}$, (3).

Definition (Cellular Witness Map). A witness map $F_{\mathcal{W}} : Y \rightrightarrows Y$ on the geometrical realization of the α -grid $Y = |\mathcal{A}|$ with landmarks L and witnesses Γ is the cellular multivalued map

$$F_{\mathcal{W}}(x) := \bigcap_{A_i \in \mathcal{A}} \{A_j \in \mathcal{A} : x \in A_i, \exists x_t \in W(l_i) \text{ such that } x_{t+1} \in W(l_j)\}. \quad (12)$$

The cellular multivalued map $F_{\mathcal{W}}$ induces a simplicial multivalued map $\mathcal{F}_{\mathcal{W}}$ in precisely the same way that $\mathcal{F}_{\mathcal{K}}$ was induced by $F_{\mathcal{A}}$, namely by (6). In other words, a simplex $\tau \in \mathcal{F}_{\mathcal{W}}(\sigma)$ whenever there are witnesses to σ that have images, under the temporal ordering of Γ , that are witnesses to τ . It is important to note that with the definition (6), we only know that $\tau \in \mathcal{K}_\alpha$; however, whenever the hypotheses of Thm. 9 are satisfied, then $\mathcal{K}_\alpha \subset \mathcal{W}_\epsilon$. Thus to guarantee $\mathcal{F}_{\mathcal{W}} : \mathcal{W}_\epsilon \rightrightarrows \mathcal{W}_\epsilon$, we assume that Γ is δ -dense on $|\mathcal{A}|$, and $\delta \leq \epsilon/2$.

Note that under the conditions of Thms. 9–10, both \mathcal{K}_α and \mathcal{W}_ϵ represent the topology of $|\mathcal{A}_\alpha|$. The fact that these complexes coincide gives us hope that $F_{\mathcal{W}}$ will carry the same information about homology as the outer approximation $F_{\mathcal{A}}$. The following theorem ensures that this indeed is the case when the original map f satisfies a Lipschitz condition on the grid.

Theorem 11. *Suppose that $Y = |\mathcal{A}_\alpha|$ is compact and f is Lipschitz on Y with constant c . Then if Γ is δ -dense on Y and $\delta \leq \frac{1}{2}\epsilon \min\{1, \frac{1}{c}\}$, $F_{\mathcal{W}}$ is an outer approximation of f .*

Proof. We need to show that for any $y \in Y$, $f(y) \in F_{\mathcal{W}}(y)$. Note that any such $y \in A_i$ for some α -cell A_i and $f(y) \in A_j$ for some other α -cell A_j . We need to show that $A_j \subset F_{\mathcal{W}}(A_i)$, or specifically, that there is an $x_t \in \Gamma$ such that $x_t \in W(l_i)$ and $x_{t+1} = f(x_t) \in W(l_j)$, where l_i and l_j are the landmarks associated with the α -cells A_i and A_j , respectively. Since Γ is δ -dense, it follows that there is $x \in \Gamma$ with $\|x - y\| \leq \delta$. Furthermore, x is at most δ closer to any landmark than y (whose closest landmark is l_i) so:

$$d(x, L) \geq d(y, l_i) - \delta, \quad (13)$$

and consequently:

$$\|x - l_i\| \leq \|x - y\| + \|y - l_i\| \leq d(x, L) + 2\delta, \quad (14)$$

Since $2\delta \leq \epsilon$, it follows that $x \in W(l_i)$. In addition, since $\|f(x) - f(y)\| \leq c\|x - y\|$ and $2c\delta \leq \epsilon$, the same reasoning as (14) leads to $f(x) \in W(l_j)$.

Note that the points y and $f(y)$ may be in multiple α -cells, but the construction above applies to each cell, and so the conclusion is unaffected. \square

We have shown that, under the conditions of Thms. 9–11:

- the witness complex computed from data has the same topology as the union of a set of α -cells that cover the data, and
- when viewed as a multivalued map on \mathbb{R}^n , $F_{\mathcal{W}}$ is an outer approximation of the dynamical system f .

Since the cellular map $F_{\mathcal{W}}$ is semicontinuous (recall §2.2), we know that whenever it is acyclic, then it is an enclosure of f . In this case, the acyclic carrier theorem implies that map on homology induced by f can be computed from any continuous selector to the witness map [Mun84, Thm. 13.3]. However, note that acyclicity cannot be guaranteed; it must be checked when the map is numerically constructed.

3.4 Computing the Homology of $\mathcal{F}_{\mathcal{W}}$

In our approach, all of the information about the topology of the attractor $\Lambda \subset X$ is contained in the simplicial complex \mathcal{W}_ϵ , so our computation of the map f_* on the homology that is induced by f relies heavily on this simplicial complex. We begin by recalling the notion of a chain map.

A chain map from one simplicial complex to another consists of a homomorphism between the vertex sets, a homomorphism between the edge sets, etc., each of which commutes with the boundary operator. Commutation implies, for example, that the boundary of the image of a k -simplex is mapped to the image of the boundary of the k -simplex. An important feature of a chain map, φ , is that it induces a well-defined map in homology, φ_* [Mun84].

Our strategy in calculating f_* is to pick an appropriate chain map, φ , so that f_* coincides with φ_* . That is, we select $\varphi : \mathcal{W} \rightarrow \mathcal{W}$ to be a *chain selector*, so that $\varphi(\sigma) \in \mathcal{F}(\sigma)$ for each $\sigma \in \mathcal{K}$. Such a selector can easily be constructed using as a piecewise linear map between the topological realizations of the simplicial complexes. That is, we consider $|\varphi| : |\mathcal{W}| \rightarrow |\mathcal{W}|$. If φ is a chain selector for the simplicial multivalued map $\mathcal{F}_{\mathcal{W}}$, then it follows that $|\varphi|$ is a continuous selector for $F_{\mathcal{W}}$ and hence, $\varphi_* = f_*$.

In summary, the strategy is as follows. To compute the homology induced by f on an isolated invariant set and hence to find its Conley index, it is sufficient to construct a cellular multivalued map $F_{\mathcal{A}}$ that encloses f . Yet computing the α -grid on a given data set and its associated cellular multivalued map $F_{\mathcal{A}}$ can be computationally expensive. In this section, we have shown how to construct a sparser simplicial complex—the witness complex $\mathcal{W}_\epsilon(\Gamma, L)$. In addition, we define two associated multivalued witness maps - the cellular map, $F_{\mathcal{W}}$, defined implicitly on $|\mathcal{A}|$ and the combinatorial simplicial map, $\mathcal{F}_{\mathcal{W}}$, defined on the finitely determined complex \mathcal{W}_ϵ . Moreover, when the hypotheses of the theorems in this section can be verified, then $\mathcal{W}_\epsilon(\Gamma, L) = \mathcal{K}_\alpha(L)$ and $F_{\mathcal{W}}$ encloses the dynamical system f . Then any continuous selector for this map will capture the homomorphism on homology f_* .

4 An example: The Hénon Map

The procedure for putting the mathematics of the previous sections into practice on time-series data from a dynamical system is as follows:

1. Given a time series $\Gamma = \{x_0, \dots, x_{T-1}\} \subset X$, which we assume lies near an attractor $\Lambda \subseteq X$, follow the procedure described on page 12 to select a set of landmarks, $L = \{l_0, \dots, l_{\ell-1}\}$,

that are evenly distributed across the attractor. These landmarks will be the vertices of a simplicial complex.

2. Choose a value for the ϵ parameter that satisfies the requirement (11) for Thm. 10 and use witness/landmark relationships to simultaneously define a simplicial complex \mathcal{W} (with vertex set L) and a simplicial multivalued map, $\mathcal{F}_{\mathcal{W}}$.
3. Pick a subset of L as a starting guess for an isolated invariant set and use Alg. 5, Alg. 6, and Alg. 8 to find an index pair $(|N|, |E|)$ for f . There are many different strategies for choosing this initial guess; if one is attempting to find periodic orbits, for instance, it makes sense to search for recurrent points in the time series and use the α -cell of the nearest landmark as the starting point for the algorithms. The important property is that the guess should be a subset of its image under the simplicial multivalued map.
4. Use a chain selector for $\mathcal{F}_{\mathcal{W}}$ to calculate $f_* : H_*(|N|, |E|) \rightarrow H_*(|N|, |E|)$.

In the rest of this section, we illustrate this procedure on Hénon’s classic map [Hén76]:

$$f(x, y) = (y + 1 - 1.4x^2, 0.3x). \quad (15)$$

Specifically, we generate a trajectory Γ of length $T = 10^5$ that starts from the initial condition $z_0 = (-0.4, 0.3)$, which is close to the attractor Λ . The trajectory is shown in Fig. 6. As a simple test of the witness map technique presented in the previous section, we use this trajectory to verify the trivial fact that f has a fixed point. Given (15), of course, a simple calculation shows that this system has *two* fixed points. Our goal is to find one of those fixed points using only the time series Γ . Note that this is a proof-of-concept example, not an exhaustive exploration of the parameter space of the algorithm. Moreover, it is simple enough that the homology calculations can be carried out by hand.

We begin by selecting a set of landmarks to approximate the attractor. Again, as a proof of principle, we simply space these landmarks evenly within the bounding box of the orbit $[-1.5, 1.5] \times [-0.4, 0.4]$. With the goal of reflecting the structure of the attractor and yet having significantly fewer landmarks than points on the orbit ($\ell \ll T$), we use a hexagonal grid with spacing $\beta = 0.05$. Indeed, retaining only those landmarks that are within β of a time-series point gives $\ell = 216$ landmarks (so $\ell \sim \sqrt{T}$), as shown in Fig. 6. This has the effect of distributing the landmarks across the attractor with enough resolution to detect some of its fractal structure.

The next step in the process is to define witness-landmark relation W_R of equation (8). Given the hexagonal geometry, the α -complex will be a clique complex when $\alpha < \beta/2$ —when it is trivially totally disconnected—or when $\alpha \geq \beta/\sqrt{3}$, the distance from a vertex to the center of the equilateral triangle of side β . Similarly, by construction, every data point is in one of the equilateral triangles formed from the landmarks, i.e., $M \leq \frac{\beta}{\sqrt{3}}$. The requirement (11) is then satisfied if we choose $\alpha = \beta/\sqrt{2}$, and

$$\epsilon \leq \left(\frac{1}{\sqrt{2}} - \frac{1}{\sqrt{3}} \right) \beta.$$

Recall that given an $\epsilon \geq 0$, a pair $(x_t, l_j) \in W_R \subset \Gamma \times L$ ($x_t \in W(l_j)$), according to (9), if and only if $\|x_t - l_j\| \leq d(x_t, L) + \epsilon$. This witness relationship serves to define a clique complex \mathcal{W}_ϵ , by (10): the edge $\langle l_i, l_j \rangle \in \mathcal{W}$ if and only if $W(l_i) \cap W(l_j) \neq \emptyset$. By varying ϵ up to the bound above

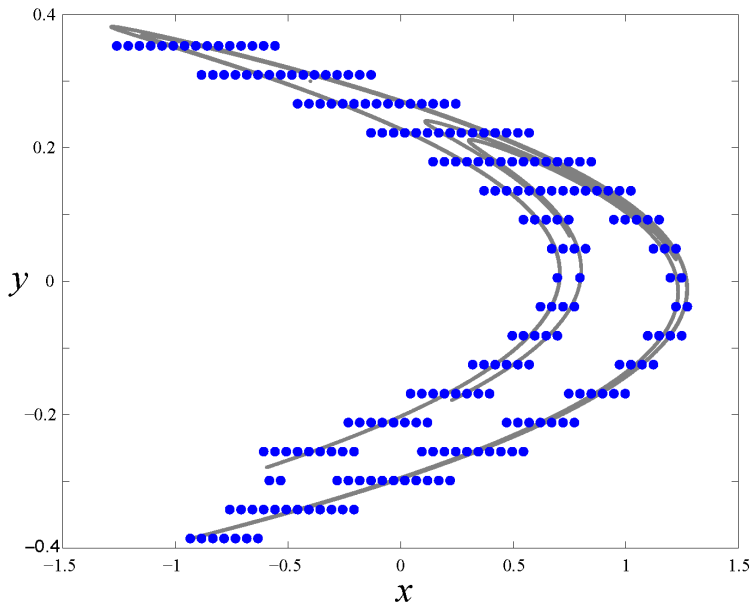


Figure 6: Time-series data, Γ , comprising 10^5 iterates of the Hénon map (15) (grey points) from an initial condition near the attractor, and the set L of 216 evenly spaced landmarks (blue circles) that approximate the attractor from which Γ was sampled. Note that the vertical and horizontal scales are different.

and looking at the resulting complexes, we finally selected $\epsilon = 0.005$; this is large enough so that the complex is connected, but small enough that the shape of the complex still reflects the primary fold in the attractor. The resulting complex is shown in Fig. 7.

Having built the witness complex, we then construct the cellular multivalued map $F_{\mathcal{W}} : |\mathcal{A}| \rightrightarrows |\mathcal{A}|$ using the witness-landmark relationships, as described by (12). Next we use the time series to search for an isolating neighborhood for $F_{\mathcal{W}}$. To apply Alg. 6, we need a guess for an isolating neighborhood. For a periodic orbit, this can be found by looking for nearly recurrent points in the time series [LK89]. Consequently, to choose an initial guess for the purpose of finding a fixed point, we can simply search for a time t that minimizes $\|x_t - x_{t+1}\|$. Following this approach, we find that $x_{39,436} = (0.6313, 0.1894)$ is a good candidate—indeed, it is close to the analytical fixed point $(x^*, y^*) \approx (0.6313544771, 0.1894063431)$. As was discussed in §2.3, the α -cell of the landmark nearest to this point gives a useful initial guess for the isolating neighborhood for Alg. 6. This is then used as the input of Alg. 8 to obtain an index pair (N, E) for the fixed point of f . The result is shown in Fig. 7.

The final step is to calculate the Conley index of the isolated invariant set that is the invariant part of $N \setminus E$. From this index, we can then infer the existence of a fixed point. We begin by taking a close look at the map $\mathcal{F}_{\mathcal{W}}$ restricted to the index pair (N, E) . The index pair is shown in Fig. 7. Recall that $F_{\mathcal{W}}$ is a map that is constant on α -cells. Though we do not need to compute these α -cells, visualizing them helps in understanding the various multivalued maps involved in this process.

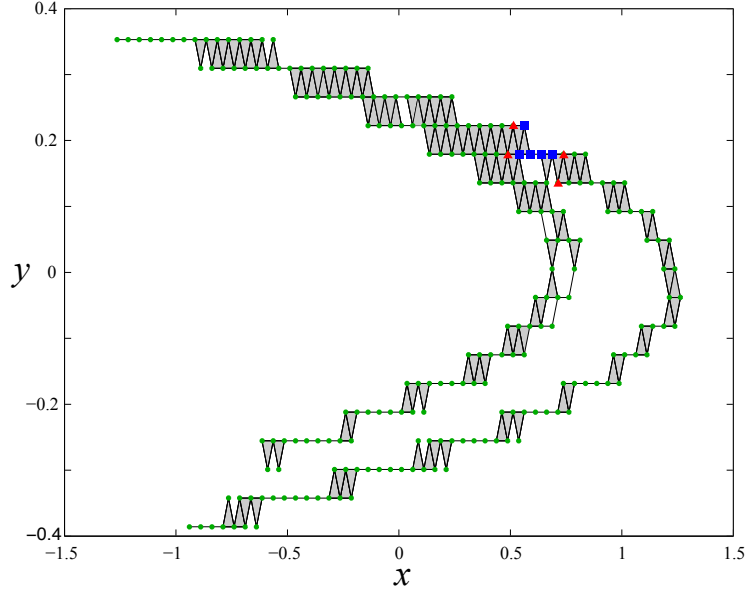


Figure 7: Witness complex and an index pair (N, E) for the fixed point of the Hénon map. The points correspond to the landmarks, L , the squares (blue) represent the isolating neighborhood $N \setminus E$ and the triangles (red) points are the exit set E . The witness complex corresponds to the landmarks, the lines, and the grey triangles.

In Fig. 8, $N = \{A_1, \dots, A_9\}$ and $E = \{A_1, A_2, A_7, A_8\}$. The blue and red landmarks are the nexuses of the α -cells that make up $N \setminus E$ and E , respectively. The map $F_{\mathcal{W}}$ restricted to the index pair can be described by the following transition matrix:

$$S = \begin{pmatrix} 0 & 0 & 0 & 0 & 0 & 0 & 0 & 0 & 0 & 0 \\ 0 & 0 & 0 & 0 & 0 & 0 & 0 & 0 & 0 & 0 \\ 1 & 0 & 0 & 0 & 0 & 1 & 1 & 0 & 0 & 0 \\ 0 & 0 & 0 & 0 & 1 & 1 & 1 & 0 & 0 & 0 \\ 0 & 0 & 1 & 1 & 1 & 0 & 0 & 1 & 1 & 0 \\ 0 & 1 & 1 & 0 & 0 & 0 & 0 & 1 & 1 & 0 \\ 0 & 0 & 0 & 0 & 0 & 0 & 0 & 0 & 0 & 0 \\ 0 & 0 & 0 & 0 & 0 & 0 & 0 & 0 & 0 & 0 \\ 0 & 0 & 0 & 0 & 0 & 1 & 1 & 0 & 0 & 0 \end{pmatrix}, \quad (16)$$

where $S_{ij} = 1$ if and only if $A_j \subset F_{\mathcal{W}}(\text{int}(A_i))$ —i.e., there is a witness of the landmark associated with A_i whose image under the shift map is a witness of the landmark associated with A_j . For example $F_{\mathcal{W}}(A_6) = A_2 \cup A_3 \cup A_8 \cup A_9$. Geometrically, this image is a disk, and is thus acyclic. Indeed, it is straightforward—if tedious—to verify from (16) that each cell maps to an acyclic set under the witness map $F_{\mathcal{W}}|_N$. Moreover, by (12), whenever $x \in A_i \cap A_j$, it has an image that is the intersection of the images of the individual cells. In this way, one can compute the images under $F_{\mathcal{W}}$ of the twelve one-dimensional simplices in the index pair. These images, inferred from (16), can be verified to be acyclic when restricted to N . Finally only one of the two-simplices in N remains in N under the map, namely $\mathcal{F}_W(\langle l_3, l_4, l_9 \rangle) = \langle l_6, l_7 \rangle$; this image has no homology. Consequently,

the map $F_{\mathcal{W}}$ is acyclic on the index pair. This condition is sufficient for our limited purpose here of verifying that f has a fixed point in N . More generally, the acyclicity of the witness maps on the entire complex could easily be automated—as is done for cubical complexes in the software package “CHomP” [Mis14].

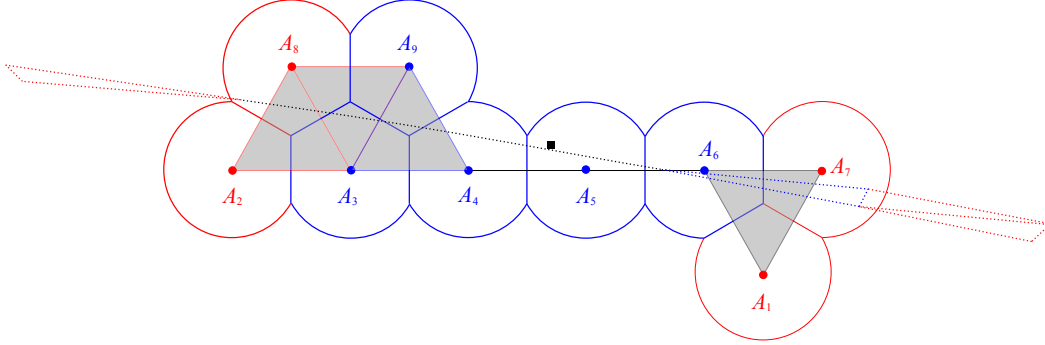


Figure 8: A pictorial representation of the α -cells associated with the index pair (N, E) (the red and blue points in Fig. 7). Also shown is the simplicial complex (grey triangles, black lines, and dots) that is the nerve of the α -cells. Dashed lines show the analytical image of the simplicial complex under the Hénon map (15). The square is the fixed point.

Now, we want to represent this index pair with a corresponding simplicial complex $\mathcal{W}(N, E)$ —specifically, the witness complex associated with the landmarks $\{l_1, \dots, l_9\}$, corresponding to α -cells $\{A_1, \dots, A_9\}$. The witness complex $\mathcal{W}(N, E)$, which is also the α -complex in this case, is pictured in Fig. 8. In order to compute the Conley index, we need a simplicial complex that represents the quotient space N/E . Since the α -cells A_1, A_2, A_7 , and A_8 make up the exit set E , we make the identification

$$l_1 \cong l_7 \cong l_2 \cong l_8 := E.$$

The resulting simplicial complex is shown in Fig. 9. The homology of the simplicial complex $\mathcal{K}(N, E)$ can easily be computed by hand in this example. In particular, the quotient space N/E consists of a single connected component so $H_{*0}(N, E) = \mathbb{Z}_2$. The quotient space has a single, nonbounding cycle:

$$\sigma = \langle E, l_3 \rangle + \langle l_3, l_4 \rangle + \langle l_4, l_5 \rangle + \langle l_5, l_6 \rangle + \langle l_6, E \rangle,$$

so $H_{*1}(N, E) = \mathbb{Z}_2$.

We are now ready to compute the Conley index of the isolating neighborhood $N \setminus E$. Specifically, we compute $f_* : H_*(N, E) \rightarrow H_*(N, E)$. As described in the previous section, the homology of f is equivalent to the homology of φ , where φ is a chain selector for $\mathcal{F}_{\mathcal{W}}$. Therefore, in order to compute the Conley index, we need to find $\varphi_*([\sigma]) := [\varphi(\sigma)]$.

The chain selector φ is defined inductively by first determining the image of each vertex in $\mathcal{K}(N, E)$ (to be enclosed by $\mathcal{F}_{\mathcal{W}}$), and then determining the image of each edge so that φ commutes with the boundary operator. In addition, recall that $\mathcal{F}_{\mathcal{W}}$ on the quotient space must be an enclosure

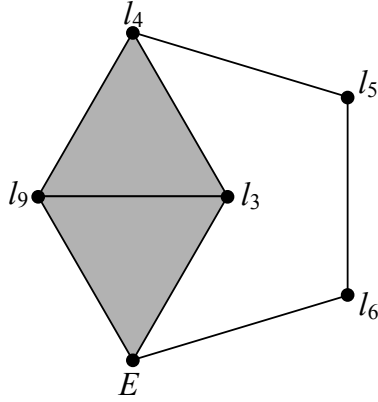


Figure 9: The quotient simplicial complex $N \setminus E$, where N is the simplicial complex shown in Fig. 8 and $E = \{l_1, l_2, l_7, l_8\}$.

of the index map f_N . We begin with the initial assignment of vertices:

$$\begin{array}{c|cccccc} \langle i \rangle & \langle E \rangle & \langle l_3 \rangle & \langle l_4 \rangle & \langle l_5 \rangle & \langle l_6 \rangle & \langle l_9 \rangle \\ \hline \varphi_0(\langle l_i \rangle) & \langle E \rangle & \langle l_6 \rangle & \langle l_5 \rangle & \langle l_3 \rangle & \langle l_9 \rangle & \langle l_6 \rangle \end{array}$$

To compute $\varphi(\sigma)$, we need to find the images of the edges in σ as well. In order for φ to be a chain selector for \mathcal{F}_W , the image of each edge, τ , must be a subset of $\mathcal{F}_W(\tau)$. Furthermore, φ must commute with the boundary operator, so we need $\varphi_0 \circ \partial_1 = \partial_1 \circ \varphi_1$. Those two conditions yield the following edge assignments:

$$\begin{array}{c|cccccc} \tau & \langle E, l_3 \rangle & \langle l_3, l_4 \rangle & \langle l_4, l_5 \rangle & \langle l_5, l_6 \rangle & \langle l_6, E \rangle \\ \hline \varphi_1(\tau) & \langle E, l_6 \rangle & \langle l_6, l_5 \rangle & \langle l_5, l_4 \rangle + \langle l_4, l_3 \rangle & \langle l_3, l_9 \rangle & \langle l_9, E \rangle \end{array}$$

It follows that $\varphi(\sigma) = \sigma$ (in \mathbb{Z}_2 homology). Since this map is not nilpotent, then it is not in the shift equivalence class of $[0]$ and thus the invariant set $S = \text{inv}(N \setminus E, f) \neq \emptyset$ [KMM04, Thm 10.91].

With this very simple example, we have illustrated that the witness complex and the associated witness map can be used to compute the Conley index for the simplest of isolating neighborhoods. We plan in the future to apply this method to more-complex and higher-dimensional dynamics.

5 Conclusions & Future Work

Computational topology is a powerful way to analyze time-series data from dynamical systems. Existing approaches to the approximation of a dynamical system on algebraic objects construct multivalued maps from the time series using cubical discretizations, then use those maps to compute the Conley indices of isolated invariant sets of cubes. The approach described in this paper, by contrast, discretizes the dynamics using a simplicial complex that is constructed from a witness-landmark relationship. A natural discretization like this, whose cell geometry is derived from the data, is more parsimonious and thus potentially more computationally efficient than a cubical complex. We then use the temporal ordering of the data to construct a map on this simplicial witness complex that we call the *witness map*. Under the conditions established in §3.3, this

witness map gives an outer approximation of the dynamics, and thus can be used to compute the Conley index of isolated invariant sets in the data.

As a proof of concept, we applied our methods to data from the classic Hénon map and located an isolating neighborhood for a fixed point of this dynamical system. There are many other potential applications. Our approach could also be used to find higher-period orbits and connecting orbits between them—a strategy that ultimately leads to rigorous verification of chaotic dynamics. Our techniques may also have significant impact in the numerical simulation of differential equations. In [MM95], numerical integration—while keeping track of the magnitude of round-off error—is used to prove that there is chaos present in the Lorenz equations [Lor63]. A key step in this proof is showing that one can construct a multivalued map that is truly an outer approximation of a given function f . Theorem 11 indicates that our techniques are appropriate for these types of proofs. The computational efficiency that the data-driven discretization confers upon the witness-map construction process should allow this approach to scale well with dimension, so it is likely that constructions based on this map could be used to generate computer-based proofs about high-dimensional differential equations. This would be a significant advance in the field.

A large body of research in the field of computational topology has revolved around the concept of *persistence* [DE95, EH08, Ghr08, Rob99]. The idea behind topological persistence is that many computations in this field depend upon simple scale parameters. For example, the α -complex of a point cloud depends upon the parameter α , the witness complex depends upon the parameter ϵ , etc. It makes sense, then, to perform these calculations over a wide range of parameter values and to search for the ranges where the topological properties remain constant. This was the rationale for the choice of the ϵ value in §4. A major area for future research is the development of a theory of persistence in the context of Conley index theory. The contribution described in this paper is a significant step in this direction.

Acknowledgment

This material is based upon work supported by the National Science Foundation under Grants #CMMI-1245947, #CNS 0720692, and #DMS-1211350. Any opinions, findings, and conclusions or recommendations expressed in this material are those of the author(s) and do not necessarily reflect the views of the National Science Foundation.

References

- [AKK⁺09] Z. Arai, W. Kailes, H. Kokubu, K. Mischaikow, H. Oka, and P. Pilarczyk. A database schema for the analysis of global dynamics of multiparameter systems. *SIAM J. Dyn. Syst.*, 8(3):757–789, 2009. <http://dx.doi.org/10.1137/080734935>.
- [Bak02] A.W. Baker. Lower bounds on entropy via the Conley index with applications to time series. *Topol. App.*, 120:333–354, 2002. [http://dx.doi.org/10.1016/S0166-8641\(01\)00083-9](http://dx.doi.org/10.1016/S0166-8641(01)00083-9).
- [BT82] R. Bott and L.W. Tu. *Differential Forms in Algebraic Topology*. Graduate Texts in Mathematics. Springer, Berlin, 1982.

- [DE95] C.J.A. Delfinado and H. Edelsbrunner. An incremental algorithm for Betti numbers of simplicial complexes on the 3-sphere. *Computer Aided Geometric Design*, 12(7):771–784, 1995.
- [DFT08] S. Day, R. Frongillo, and R. Trevino. Algorithms for rigorous entropy bounds and symbolic dynamics. *SIAM J. Appl. Dyn. Syst.*, 7(4):1477–1506, 2008. <http://dx.doi.org/10.1137/070688080>.
- [DJM04] S. Day, O. Junge, and K. Mischaikow. A rigorous numerical method for the global analysis of infinite-dimensional discrete dynamical systems. *SIAM J. Appl. Dyn. Syst.*, 3:117–160, 2004. <http://dx.doi.org/10.1137/030600210>.
- [Dow52] C.H. Dowker. Homology groups of relations. *Ann. of Math*, 56(1):84–95, 1952.
- [dSC04] V. de Silva and E. Carlsson. Topological estimation using witness complexes. In M. Alexa and S. Rusinkiewicz, editors, *Eurographics Symposium on Point-Based Graphics (2004)*. The Eurographics Association, Zurich, 2004.
- [Eas98] R.W. Easton. *Geometric Methods for Discrete Dynamical Systems*. Oxford University Press, 1998.
- [Ede95] H. Edelsbrunner. The union of balls and its dual shape. *Discrete Comput. Geom.*, 13:415–440, 1995. <http://dx.doi.org/10.1007/BF02574053>.
- [EH08] H. Edelsbrunner and J. Harer. Persistent homology: A survey. In J.E. Goodman, J. Pach, and R. Pollack, editors, *Surveys on Discrete and Computational Geometry: Twenty Years Later*, volume 453 of *Contemporary Mathematics*, pages 257–282. American Mathematical Society, Providence, 2008. <http://dx.doi.org/10.1090/conm/453/08802>.
- [EM92] H. Edelsbrunner and E.P. Mücke. Three-dimensional alpha shapes. In *Proceedings of the 1992 Workshop on Volume Visualization*, pages 75–82. ACM, 1992.
- [FBF77] J. H. Friedman, J. L. Bentley, and R. A Finkel. An algorithm for finding best matches in logarithmic expected time. *ACM Trans. Math. Software*, 3:209–226, 1977.
- [Ghr08] R. Ghrist. Barcodes: The persistent topology of data. *Bull. AMS*, 45(1):61, 2008. <http://dx.doi.org/10.1090/S0273-0979-07-01191-3>.
- [Hén76] M. Hénon. A two-dimensional mapping with a strange attractor. *Comm. Math. Phys.*, 50(1):69–77, 1976. <http://dx.doi.org/10.1007/BF01608556>.
- [KMM04] T. Kaczynski, K. Mischaikow, and M. Mrozek. *Computational Homology*, volume 157 of *Applied Mathematical Sciences*. Springer-Verlag, New York, 2004.
- [KMV05] W.D. Kalies, K. Mischaikow, and R. VanderVorst. An algorithmic approach to chain recurrence. *Found. Comput. Math.*, 5(4):409–449, 2005. <http://dx.doi.org/10.1007/s10208-004-0163-9>.

- [LK89] D.P. Lathrop and E.J. Kostelich. Characterization of an experimental strange attractor by periodic orbits. *Phys. Rev. A*, 40:4028–4031, 1989. <http://link.aps.org/doi/10.1103/PhysRevA.40.4028>.
- [Lor63] E.N. Lorenz. Deterministic nonperiodic flow. *J. Atmos. Sci.*, 20(2):130–141, 1963. [http://dx.doi.org/10.1175/1520-0469\(1963\)020<0130:DNF>2.0.CO;2](http://dx.doi.org/10.1175/1520-0469(1963)020<0130:DNF>2.0.CO;2).
- [Mis14] K. Mischaikow. CHomP: Computational homology project, 2014. <http://chomp.rutgers.edu>.
- [MM95] K. Mischaikow and M. Mrozek. Chaos in the Lorenz equations: A computer-assisted proof. *Bull. AMS*, 32(1):66–72, 1995. <http://dx.doi.org/10.1090/S0273-0979-1995-00558-6>.
- [MM02] K. Mischaikow and M. Mrozek. Conley index theory. *Handbook of Dynamical Systems*, 2:393–460, 2002.
- [MMRS99] K. Mischaikow, M. Mrozek, J. Reiss, and A. Szymczak. Construction of symbolic dynamics from experimental time series. *Phys. Rev. Lett.*, 82(6):1144–1147, 1999. <http://link.aps.org/doi/10.1103/PhysRevLett.82.1144>.
- [MMSR97] K. Mischaikow, M. Mrozek, A. Szymczak, and J. Reiss. From time series to symbolic dynamics: An algebraic topological approach. Technical report, Georgia Inst. of Tech., December 1997 1997. <http://www.math.rutgers.edu/%7Emischaik/papers/tseries.ps>.
- [Mro99] M. Mrozek. An algorithmic approach to the Conley index theory. *J. Dynamics and Diff. Eq.*, 11(4):711–734, 1999. <http://dx.doi.org/10.1023/A:1022615629693>.
- [Mun84] J.R. Munkres. *Elements of Algebraic Topology*. Benjamin/Cummings, Menlo Park, 1984.
- [Rob99] V. Robins. Towards computing homology from finite approximations. *Topology Proceedings*, 24(1):503–532, 1999. <http://at.yorku.ca/b/a/a/k/28.htm>.
- [Wu62] W.T.S. Wu. On a theorem of Leray. *Chinese Math*, 2:398–410, 1962.
- [ZC05] A.J. Zomorodian and G. Carlsson. Computing persistent homology. *Disc. Comp. Geom.*, 33:249–274, 2005. <http://dx.doi.org/10.1007/s00454-004-1146-y>.
- [Zom10] A.J. Zomorodian. Fast construction of the Vietoris-Rips complex. *Computers & Graphics-UK*, 34(3):263–271, 2010. <http://dx.doi.org/10.1016/j.cag.2010.03.007>.